Atmospheric Research 204 (2018) 110–127

Contents lists available at ScienceDirect

Atmospheric Research

journal homepage: www.elsevier.com/locate/atmosres

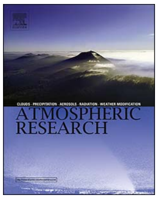

Assessment of 1D and 3D model simulated radiation flux based on surface measurements and estimation of aerosol forcing and their climatological aspects

T. Subba[a], M.M. Gogoi[c], B. Pathak[a,b,*], Ajay P.[a], P.K. Bhuyan[a], F. Solmon[d]

[a] *Centre for Atmospheric Studies, Dibrugarh University, Dibrugarh 786004, India*
[b] *Department of Physics, Dibrugarh University, Dibrugarh 786004, India*
[c] *Space Physics Laboratory, Vikram Sarabhai Space Centre, ISRO, Trivandrum 695022, India*
[d] *Laboratoir d'Aerologie, Observatoir Midi-Pyrenees, Toulouse, France*

ARTICLE INFO

Keywords:
Solar radiation
SBDART
RegCM4.4
Surface albedo
Aerosol radiative forcing efficiency
Heating rate

ABSTRACT

Ground reaching solar radiation flux was simulated using a 1-dimensional radiative transfer (SBDART) and a 3-dimensional regional climate (RegCM 4.4) model and their seasonality against simultaneous surface measurements carried out using a CNR4 net Radiometer over a sub-Himalayan foothill site of south-east Asia was assessed for the period from March 2013–January 2015. The model simulated incoming fluxes showed a very good correlation with the measured values with correlation coefficient $R^2 \sim 0.97$. The mean bias errors between these two varied from $-40\ \mathrm{W\,m^{-2}}$ to $+7\ \mathrm{W\,m^{-2}}$ with an overestimation of 2–3% by SBDART and an underestimation of 2–9% by RegCM. Collocated measurements of the optical parameters of aerosols indicated a reduction in atmospheric transmission path by ~20% due to aerosol load in the atmosphere when compared with the aerosol free atmospheric condition. Estimation of aerosol radiative forcing efficiency (ARFE) indicated that the presence of black carbon (BC, 10–15%) led to a surface dimming by $-26.14\ \mathrm{W\,m^{-2}}\,\tau^{-1}$ and a potential atmospheric forcing of $+43.04\ \mathrm{W\,m^{-2}}\,\tau^{-1}$. BC alone is responsible for > 70% influence with a major role in building up of forcing efficiency of $+55.69\ \mathrm{W\,m^{-2}}\,\tau^{-1}$ (composite) in the atmosphere. On the other hand, the scattering due to aerosols enhance the outgoing radiation at the top of the atmosphere ($\mathrm{ARFE_{TOA}} \sim -12.60\ \mathrm{W\,m^{-2}}\,\omega^{-1}$), the absence of which would have resulted in $\mathrm{ARFE_{TOA}}$ of $\sim +16.91\ \mathrm{W\,m^{-2}}\,\tau^{-1}$ (due to BC alone). As a result, ~3/4 of the radiation absorption in the atmosphere is ascribed to the presence of BC. This translated to an atmospheric heating rate of $\sim 1.0\ \mathrm{K\,day^{-1}}$, with $\sim 0.3\ \mathrm{K\,day^{-1}}$ heating over the elevated regions (2–4 km) of the atmosphere, especially during pre-monsoon season. Comparison of the satellite (MODIS) derived and ground based estimates of surface albedo showed seasonal difference in their magnitudes ($R^2 \sim 0.98$ during retreating monsoon and winter; ~0.65 during pre-monsoon and monsoon), indicating that the reliability of the satellite data for aerosol radiative forcing estimation is more during the retreating and winter seasons.

1. Introduction

Modeling the solar radiation and accurate estimation of the surface reaching fluxes is challenging due to varying geographical parameters such as topographic shadowing and reflection from the inclined surfaces (Austin et al., 2013). This is further complicated by the presence of atmospheric components, e.g., aerosols and clouds. The variation in cloudiness plays the major role in the uncertainties regarding the simulation of solar radiation reaching the ground (Kambezidis et al., 2017 and references therein). Aerosols interact with the incoming solar radiation and upward terrestrial radiation thus, modifying the incoming solar photons (through scattering and absorption) penetrating into the atmosphere in both shortwave (SW, $\lambda < 4\ \mu\mathrm{m}$) and the long-wave (LW, $4\ \mu\mathrm{m} < \lambda < 100\ \mu\mathrm{m}$) range. These alterations affect the human comfort and involuntarily shape up the regional and global climate. Recent studies indicated that the contribution of aerosols in the Earth's energy budget estimation is highly uncertain due to the complex aerosol-climate feedback mechanisms associated with distinct spatio-temporal variability of the sources, emission strengths and sinks (Ohmura, 2006; Wild, 2009; Qian et al., 2007; IPCC, 2013). Several studies have been made, both regionally and globally to address this complex problem using various techniques and platforms to understand the impact of atmospheric aerosols in perturbing the global radiation budget, surface temperature, cloud properties and precipitation patterns (Stanhill,

---

[*] Corresponding author.
E-mail address: binita@dibru.ac.in (B. Pathak).

https://doi.org/10.1016/j.atmosres.2018.01.012
Received 2 November 2016; Received in revised form 15 September 2017; Accepted 16 January 2018

1995; Satheesh and Ramanathan, 2000; Satheesh et al., 2006; Ramanathan et al., 2001b; Kaufman et al., 2005; Lau and Kim, 2006; Yu et al., 2006; Remer et al., 2009). It has been reported that during the last century, the aerosol loading has drastically increased (Boucher and Haywood, 2001; Wild, 2009) and the atmospheric constitution has changed due to tropical urbanization. This has influenced the moisture and energy balance of the urban and rural biosphere (Trusilova and Churkina, 2008), affected local and regional circulation and developed long lasting haze events (Zhang et al., 2013; Wang et al., 2015).

In addition to the direct impact of aerosols on radiation, underlying surface albedo of the planet also plays an important role in the energy balance of the Earth-atmosphere system. According to IPCC (2013), $\sim -0.2\,\mathrm{W\,m^{-2}}$ change in the SW flux has been induced due to alteration of albedo from completely vegetation covered state to the era of industrialization. A reduction in radiation energy absorbed at the surface leads to decrease in the surface latent heat and sensible heat flux and hence, influences the convection and precipitation patterns (Dirmeyer and Shukla, 1994). However, the surface albedo also exhibits strong spatial and temporal variation depending upon the seasonal dynamics, soil-vegetation cover, canopy chemistry and landscape (Roman et al., 2009). The changes in surface albedo are found to be crucial for executing the biosphere models and to understand the land surface climate (Disney et al., 2004).

At this juncture, it is important to note that the estimation of aerosol radiative forcing (ARF) is not accurate if the simulated (using radiative transfer or regional climate models) radiation fluxes are not validated against measurements. The ARF estimation deviates further if the information of surface albedo is inaccurately fed into the radiative transfer models. Even though MODIS (Moderate–resolution Imaging Spectroradiometer) BRDF (Bidirectional Reflectance Distribution Function)/albedo products have been widely used to retrieve the high quality surface reflectance anisotropy over diverse land surfaces since 2000 (Schaaf et al., 2002; Brun et al., 2015), the comparison of these satellite products with the field measurements are limited.

Viewed against the above backdrops, the long term continuous measurement of surface radiation fluxes were examined and used to validate the model simulations. Collocated and simultaneous measurements of aerosol parameters, along with the validated radiation fluxes are used for the estimation of ARF. The observational site Dibrugarh (DBR, 27.3° N, 94.6° E, 111 m above the mean sea level) (Fig.1), in the sub-Himalayan foot-hill region of north-east India is strategically located for the study of the south-east Asian aerosol. Even though the region is endowed with dense vegetation cover and minimal industrial and anthropogenic activity, earlier investigations have shown considerable aerosol loading over and around the observational site (Pathak et al., 2016), mainly due to the influx of minerals and carbonaceous aerosols from distinct local and regional sources. The topography of the north-eastern region of India (NER) is such that it is encircled by the vast Himalayan range and Tibetan Plateau to the north, Garo-Khasi-Jayantia and Naga hills to the south and mountains of Yanan to the east. The unwrapped western corridor allows the unrestricted advection of transported anthropogenic aerosols from the Indo-Gangetic Plain (IGP), the Indian Mainland and Bangladesh, desert dusts from Africa, western India/Asia and marine aerosols from Bay of Bengal (BoB) (Gogoi et al., 2009, 2011; Pathak et al., 2010, 2016). Besides, the seasonal biomass burning activities in the nearby hills also contribute to the aerosol abundance over the region. With respect to the climatic conditions, NER follows distinctive sub-tropical weather pattern with cool and dry winter (December–February) (DJF) followed by hot and humid pre-monsoon (March–May) (MAM) and prolonged period of rainy season. Calm north easterly during DJF and retreating monsoon (October–November) (ON) and calm westerlies during MAM with strong south westerlies during monsoon (June–September) (JJAS).

In the present study, we have used the surface radiative fluxes measured using CNR4 net Radiometer for the period from March 2013–January 2015. Collocated aerosol parameters [e.g., aerosol optical depth (AOD) and black carbon (BC) mass concentrations] were obtained for the period from 2008 to 2014. This is the first time approach in the selected region to incorporate the continuous long term data sets for the validation of simulated fluxes along with the MODIS albedo product, which provides a realistic picture of the assessment of atmospheric warming and surface cooling due to aerosols. The study can eventually help in the estimation of the impact of aerosols on aerosol environment and regional climate over the south-east Asian region.

2. Database and analysis

2.1. Measurements of SW flux at the Earth's surface

Continuous measurements of the surface reaching SW radiation was carried out using Kipp and Zonen CNR4 net radiometer, mounted on a 2 m tall rigid platform above the ground. Much away from the wayside, in the field of uninterrupted homogeneous cover, the pair of pyranometer and pyrgeometer exposed entirely towards the sky (i.e. $2\pi^2$ field of view) provided the SW (0.3 to 3.0 μm) solar and LW (4.5 to 42 μm) far infrared radiations respectively. The relative uncertainty in the net radiometers' measurements was estimated within 2–5% (Das et al., 2009; Li et al., 2010). In the present study, the SW net radiations have been examined for the two consecutive years, consisting of clear sky data for 345 days out of the 600 days of measurements. The net shortwave radiation (SW_{NET}) is deduced from the energy budget equation as:

$$SW_{NET} = SW_{IN} - SW_{OUT} \tag{1}$$

where, SW_{IN} and SW_{OUT} are incoming and outgoing shortwave radiations, respectively. Both SW_{IN} and SW_{OUT} are normalized for normal incidence conditions, following relation (Iqbal, 1983):

$$\text{Normalized flux} = \frac{\text{Measured flux}}{E_o[\sin\varphi\ \sin\delta + \cos\varphi\ \cos\delta\ \cos(Ha)]} \tag{2}$$

where, E_o is the eccentricity correction factor on account of the elliptical Earth's orbit, δ the solar declination (the angle describing the position of the sun relative to the plane of the celestial equator), φ the latitude of the measurement site and Ha the hour angle, which are calculated as:

$$Eo = \left(\frac{r_0}{r}\right)^2 = 1.000110 + 0.034221\cos(\tau) + 0.001280\ \sin(\tau) + 0.000719\ \cos(2\tau) + 0.000077\ \sin(2\tau) \tag{3}$$

$$\delta = [0.006918 - 0.399912\ \cos(\tau) + 0.070257\ \sin(\tau) - 0.006758\cos(2\tau) + 0.000907\ \sin(2\tau) - 0.002697\ \cos(3\tau) + 0.00148\ \sin(3\tau)]180 \tag{4}$$

In Eq. (3) r and r_o are instantaneous and mean (~1 AU) Sun-Earth distance, τ the day angle which is calculated as:

$$\tau = \frac{2\pi(d_n - 1)}{365}, \tag{5}$$

where 'd_n' is the Julian day number in a year.

Hour angle (Ha) describes the position of the sun with respect to solar noon, which changes 15 degree per hour with positive values during the morning, reduces to zero at solar noon and becomes increasingly negative as the afternoon progresses. The hour angle H_a is calculated following Vardavas and Taylor (2006) as:

$$H_a = \text{arcos}\,(-\tan\varphi\ \tan d) \tag{6}$$

While calculating the hour angle (i.e., the current position of the Sun), the discrepancy between the apparent (true) solar time and solar mean time is taken into account, which is known as equation of time (E_t) representing the angular offset of the Sun from its mean position on the celestial sphere as viewed from Earth. While the apparent solar time directly tracks the motion of the sun, mean solar time tracks a